4-22-2020

Analysis of Cryptotephra at Whitney Mesa Nature Preserve, Henderson, Nevada

Alex Newsom
newsoa1@unlv.nevada.edu

ANALYSIS OF CRYPTOTEPHRA AT WHITNEY MESA NATURE PRESERVE, HENDERSON, NEVADA

By

Alex Newsom

Honors Thesis submitted in partial fulfillment for the designation of

Research and Creative Honors

Geoscience Department

Committee Members:

Eugene Smith

Racheal Johnsen

Simon Jowitt

Lisa Menegatos

College of Sciences

University of Nevada, Las Vegas

May, 2020

Abstract

Cryptotephra (small volcanic shards ranging 20-80 microns in size) were discovered within Unit X of the Las Vegas Formation at Whitney Mesa Nature Preserve, Henderson, Nevada. Cryptotephra are deposited soon after a volcanic eruption and can be used as a dating tool to create narrow time constraints for surrounding sediments. Cryptotephra have many applications but are mainly useful as a dating tool. Their study has important implications for the understanding of the timing of palaeoclimatological and paleoenvironmental events as well as for archaeological studies to date important events in human history.

The Whitney Mesa cryptotephra were correlated with the Bishop Tuff, dated at 766 ka. The Las Vegas Formation underlies much of the Las Vegas Valley but, due to expansive urbanization, it is now best exposed at Tule Springs Fossil Beds National Monument, Whitney Mesa Nature Preserve, and Charlie Frias Park. The Las Vegas Formation is divided into five main units with an E member on top and an X member as the base. The age of Unit X (the subject of this study) is poorly known, with previous dates ranging from 232 to 573 ka. The discovery of cryptotephra and correlation with Bishop Tuff provide the first precise date for Las Vegas Formation Unit X. This work was accomplished using sediment sample collection, wet-lab techniques at UNLV's Cryptotephra Laboratory for Archaeological and Geologic Research (CLAGR), petrographic microscope analysis, and electron microprobe geochemical analysis at UNLV's Electron Microanalysis and Imaging Laboratory (EMiL).

Acknowledgements

I would like to thank Gene and Racheal for opening their experiences to me and sharing their knowledge with me, as well as helping me through this process, while simultaneously acting as inspiring role models.

I want to thank Simon Jowitt and Lisa Menegatos as well for being there for me the past few years, helping me through various obstacles, and providing me helpful advice which will help me grow as a person and as a researcher.

Thank you to Minghua Ren for helping us in EMiL, Alex for his guidance and liveliness within CLAGR, and my friends who would listen to my geologic rants throughout these semesters.

Table of Contents

Figures

Tables

Introduction

Cryptotephra, also known as ultra-distal tephra, micro-tephra, and non-visible tephra, are classified as volcanic glass shards ranging in size between 20 and 80 microns. The correlation of cryptotephra to a known volcanic event provides a dating tool, known as tephrochronology, that helps fill in gaps within the geologic time scale that are difficult to date using traditional radiocarbon or luminescence techniques (Lowe et al., 2012; Lane et al., 2014; Lowe & Alloway, 2015). Cryptotephra studies also aid the understanding of volcanic processes, ash transport, future volcanic events, and potential hazards (Lowe et al., 2012; Lane et al., 2014; Lowe & Alloway, 2015).

Lane et al. (2014; 2017) detail the development of cryptotephra research, such as dating methods and interdisciplinary uses of cryptotephra studies as well as describe a society focused on tephra studies: INTAV (International Focus Group on Tephrochronology and Volcanism). Other researchers in the cryptotephra field, such as Sarna-Wojcicki et al. (1987), Knott et al. (2018) and Spano et al. (2017), have all furthered the understanding of cryptotephra in the Western United States by establishing a stratigraphic framework of tephra units and providing geochemical data useful for identifying unknown tephra and cryptotephra units. Springer and colleagues' research in the Western United States has also been highly beneficial for cryptotephra analysis. Their detailed dating of the Las Vegas Formation in Tule Springs Fossil Beds National Monument establishes a chronologic framework for this cryptotephra study (Springer et al., 2015; Springer et al., 2018a,b; Smith et al., 2019).

This Honor's thesis deals with the search for cryptotephra within the Las Vegas Formation at Whitney Mesa in Henderson Nevada. The study area was selected because

it contains excellent exposures of the lowermost prat of the Pleistocene to Holocene Las Vegas Formation. The primary goal of this thesis involved searching for cryptotephra to provide a precise date for the Las Vegas Formation at Whitney Mesa.

Geologic Background

Tephra Definition and Transport

A volcanic eruption releases tephra of varying sizes and classifications (i.e. ash, bombs, cryptotephra) that can be carried up through the layers of the atmosphere, passing through the more active troposphere and into the stratosphere (Schmincke, 2004). How much energy is necessary for columns to reach stratospheric heights depends on the geographic location of the volcanic complex, with a focus on latitude. For instance, volcanoes at higher latitudes such as Sarychev, Kamchatka Russia, need a far lower amount of energy to inject ash, particulates, and gases into the stratosphere compared to volcanoes at lower latitudes, like Cotopaxi, Ecuador (Schmincke, 2004). The key component of such injection is the gaseous products of the eruption, which traverse the globe for up to three years, forming different compounds, releasing ozone, and altering global circulation and temperature patterns. Tephra, on the other hand, are more likely to deposit within the first initial days or weeks and cannot maintain atmospheric travel for nearly as long as the volcanic gases. The smaller the particle, the longer it can remain suspended and thus the farther it can travel. Cryptotephra, having a size range between 20 and 80 microns, can remain in the atmosphere for months, thus dispersing globally (Folch, 2012).

Another key factor to consider when assessing transportation processes and even deposition of cryptotephra is a volcano's Volcanic Explosivity Index (VEI). This focuses

on the volume of erupted tephra, while also taking into account columnar height and other characteristics of an eruption (Appendix 1). This scale ranges from 0 to 8, with 0 ejecting less than 10,000 m^3 of tephra and 8 ejecting more than 1,000 km^3 of tephra (U.S.G.S. Glossary). For context, the Long Valley Caldera event that produced the Bishop tuff around 766 ka is thought to have had a VEI ranging between 5 and 7.5, producing around 500 km^3 of tephra, while the Toba event 74 ka had a VEI of 8 and released 2,800 km^3 of tephra (Izett, 1981; Izett et al., 1988; King).

By combining the geographic location of a volcanic eruption and its VEI, we can more effectively propose where tephra and cryptotephra may deposit. Working backwards from this, we can more accurately correlate source volcanoes of cryptotephra from where they were deposited.

Cryptotephra as a Dating and Archaeological Tool

Cryptotephra have the advantage of defining precise isochrons due to their ability to be correlated with a single volcanic event, which will have specific, narrow, known age ranges. Consequently, cryptotephra is used to precisely date sediments at archaeological sites and help advance archaeological studies of early modern humans and civilizations. Though many anthropological and archaeological studies utilize carbon-dating techniques, studies of early modern humans extend much farther into the past than the 50-30 ka limit of carbon-dating; one such subfield being that of early modern humans in South Africa, which exceed 100 ka (Smith et al., 2018). Due to the restrictions of carbon-dating, cryptotephra horizons are used in conjunction with speleothem data and zircon dating to link different archaeological sites temporally and socially (Blockley et al., 2007; Zanchetta et al., 2011; Hirniak et al., 2019). By placing separate sites within

the same narrow timeframe, we can determine whether these sites belonged to the same society while also identifying other social connections between these societies.

Cryptotephra can be found within a diverse range of environments, including ice-cores, lacustrine deposits, peat bogs, and wetlands, with some cases of preservation in desert environments as well (Mark et al., 2014; Giaccio et al., 2017; Davies et al., 2018; Wastegard et al., 2018; Hirniak et al., 2019). The diverse yet simultaneously specific range of environments that offer potential preservation of cryptotephra allows tephrochronology to be used not only for archaeological studies but also for modern and palaeoclimatological studies, acting as a key component in understanding significant climatic events (Wastegard et al., 2018).

The correlation of volcanic eruptions and climactic events such as temperature fluctuations is key to understanding palaeoclimatological processes and times of crises throughout human history. One example includes the Seventeenth-Century Crisis where volcanic eruptions were correlated with cold spells and contributed to the cycle of drought, famine, pestilence, and depopulation of humans (Parker, 2013). Another example of using cryptotephra to link paleoclimate changes with human evolution is seen during the collapse of Mediterranean civilizations during the Bronze age, also correlating volcanic eruptions with cold spells, droughts, and famines (Blockley et al., 2007; Roberts et al., 2011; Zanchetta et al., 2011).

The significance of cryptotephra in the understanding of early civilizations within the Las Vegas Valley is yet to be explored. Some of the first evidences of human civilization in the Las Vegas Valley was published in 1933 by G.G. Simpson, concerning

an anthropogenically worked obsidian flake found in the vicinity of various Pleistocene sediments and mammalian fossils at Tule Springs (Simpson, 1933; Sellards, 1960).

The Las Vegas Formation

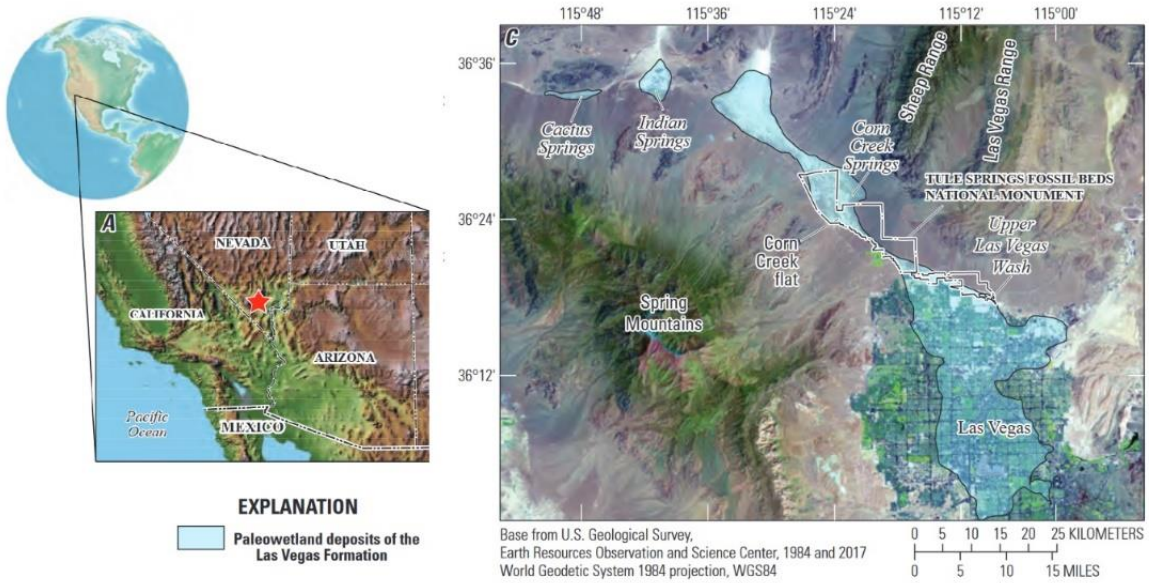

Figure 1: Map and model of the Las Vegas Valley and Las Vegas Formation, taken from page 2 of Springer et al., 2018 .

The Pleistocene to Holocene Las Vegas Formation consists of 17 distinct beds that are divided into five units labeled X to E, moving upwards (Springer et al., 2018). The beds within units are given numerical labels such as D2 or E1. The Las Vegas Formation well exposed in the Tule Springs Fossil Beds National Monument (Figure 1) represents a paleowetlands environment formed by hydrologic processes and groundwater discharge cycles (GWD). These GWD cycles help define various stratigraphic units. The stratigraphy of the Las Vegas Formation is dominated by sandstones, siltstones, reworked carbonate nodules, groundwater carbonates, fine-grained alluvial fan sediments, developed paleosols, and various fossils including Colombian mammoths (Rowland et al., 2015; Springer et al., 2017; Springer et al., 2018).

Unit X: Whitney Mesa

Figure 2: Maps of exposed portions of Unit X, made with Google Earth and MS Paint. ***A:*** *Whitney Mesa Nature Preserve, Henderson* ***B****: Charlie Frias Park, Las Vegas*

Whitney Mesa is located in the eastern part of the Las Vegas Valley (Figure 2) and was formed by erosion of the footwall of the Whitney Mesa fault, a segment of the Las Vegas Valley Fault System (LVVFS) (Springer et al., 2018; dePolo et al., 2008; Taylor, 2003). Unit X of the Las Vegas Formation is well exposed along the east facing escarpment of Whitney Mesa (Springer, personal communication) and has been informally divided into four beds, X1 – X4 (Smith, personal communication). Bed X1 forms slopes at the base of Whitney Mesa and is composed of fine-grained silt and clay (Figure 3). Bed X2 is well lithified and forms a 10 m high vertical escarpment. This bed

is composed of carbonate sedimented siltstone and clay interbedded with 1 to 3 m thick conglomerate units. Bed X3 is a slope former and composed of fine-grained silts and clays, similar in lithology to bed X1. The Unit X section is capped by bed X4; a caliche and carbonate cemented siltstone. A thin fanglomerate overlies bed X4 and is characterized by abundant blocks of basalt. Springer et al. (2018) reported thermoluminescence dates of 399-226 ka, 379-232 ka (Lundstrom et al., 1998; Page et al., 2005) and 573±52 ka taken from surficial samples of bed X4. Unit X lithology at Whitney Mesa is similar to that found in Unit X at Tule Springs Fossil Beds National Monument (Springer et al., 2018) and at Charlie Frias Park in Clark County at the intersection of Tropicana and Decatur Avenues (Springer, personal communication).

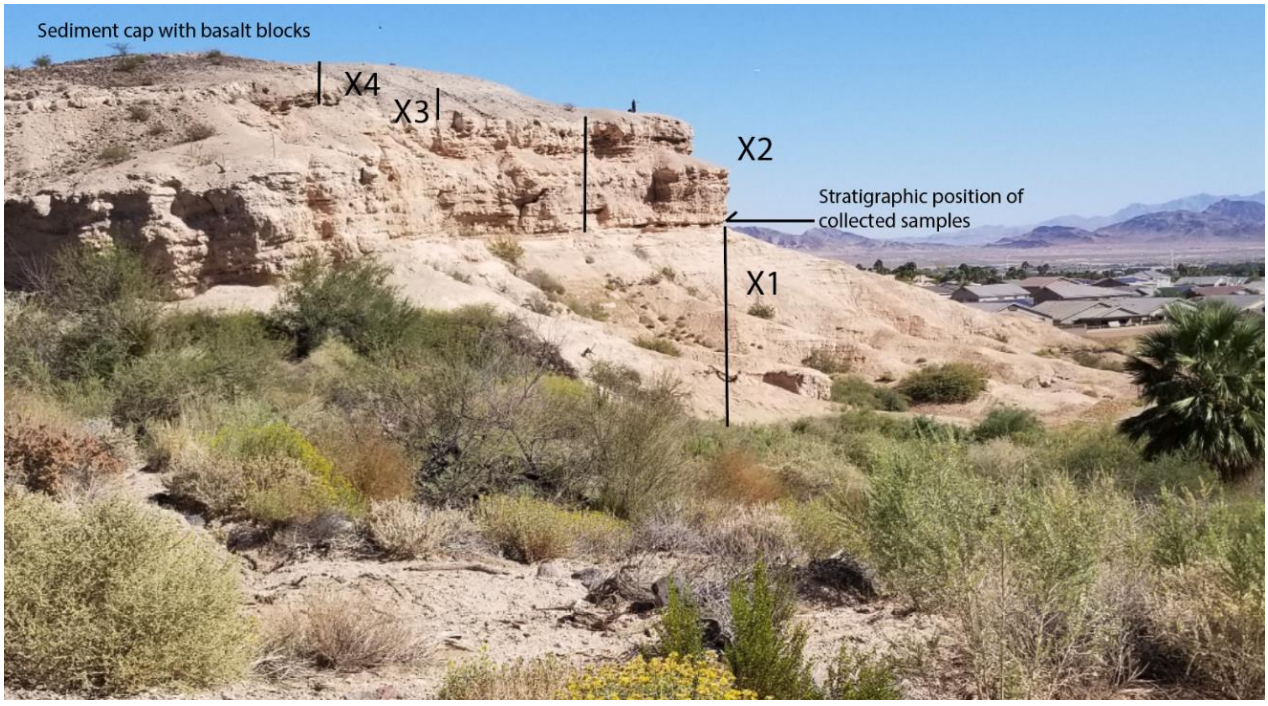

Figure 3: Stratigraphic sequence at Whitney Mesa. Cryptotephra samples were collected from the base of bed X2. Profile created by Gene Smith.

Previous Cryptotephra Studies

Cryptotephra in the form of glass shards have recently been discovered in the Las Vegas Formation at Tule Springs in Unit D2 (Smith et al., 2019). Shards are sparse (<10 shards/gram) and small (60-100 microns) and display blocky and cuspate shapes. Major element chemistry by electron microprobe indicated that the shards are high-silica rhyolite (>75 wt. % SiO_2) with FeO < 1 wt. %, providing a unique major element signature that correlates to Wilson Creek tephra that erupted from the Mono Craters in eastern California. The Wilson Creek section contains 19 tephra layers that are indistinguishable using major elements but have distinctive trace element signatures. Smith et al. (2019) suggested based on major and trace elements that shards in unit D2 correlate with Wilson Creek tephra #15 (32 ka).

Research Questions

Our primary question was whether there are cryptotephra shards within the Las Vegas Formation at Whitney Mesa. We were successful in answering this question by discovering four shards at Whitney Mesa within Unit X. Our next research question was which known volcanic eruption was responsible for the recently discovered shards? By correlating the found shards with known volcanic events, we were able to more precisely date the formation in which they were found.

Methodology

Potential collection sites were identified on October 1st, 2019, when our team (Alex Newsom, Racheal Johnsen, Eugene Smith) went to Whitney Mesa Nature Preserve. The sample collection process began November 19th, 2019, at Whitney Mesa Preserve where we collected 24 samples in 10 cm increments from the sediment column exposed

along the cliffside of the section, with a 25th sample being collected on the top. The sediments were mainly sands and clays with pebbles interspersed throughout and one conglomerate layer at 140-215 cm where no samples were collected. Other characteristics observed included caliche along top sections and fallen or remobilized deposits along basal sections from erosional and weathering processes.

At UNLV's Cryptotephra Laboratory for Archaeological and Geological Research (CLAGR) in the Lily Fong Geoscience building, the samples were processed through a variety of wet-lab techniques. The samples were measured out into approximate 1-gram samples and placed in beakers with hydrochloric acid (HCl) to dissolve carbonaceous material. Once the HCl processing finished, hydrogen peroxide (H_2O_2) was added until no further activity (i.e. fizzing) was observed. The sediments were then rinsed with water (that had undergone reverse osmosis filtration) and sieved in a mesh tower using 20- and 80-micron disposable mesh. These ideally sized samples were then processed with liquid metatungstate (LMT) between 2.2 g/cm^3 and 2.5 g/cm^3. These samples underwent 15 minutes in the centrifuge after each LMT treatment to allow cryptotephra shards to be separated to the top. Next, these samples were poured into medium filters within the original beakers and rinsed. A more detailed flow chart is provided in Appendix 2.

The resulting shards were then mounted in epoxy rounds and polished 500, 800, and then 1200 grit size pads before being polished with diamond sprays of 6, 3, and 1 microns. Using a petrographic microscope, rounds were analyzed to interpret whether there were shards collected. Of those processed and analyzed, samples 19WM-1, 19WM-11, 19WM-12, and 19WM-13 were noted to have potential cryptotephra shards (Figure

4). Throughout this, two samples were re-processed (19WM-9 and 19WM-16) due to lack of sufficient end results; no further shards were recovered.

Results

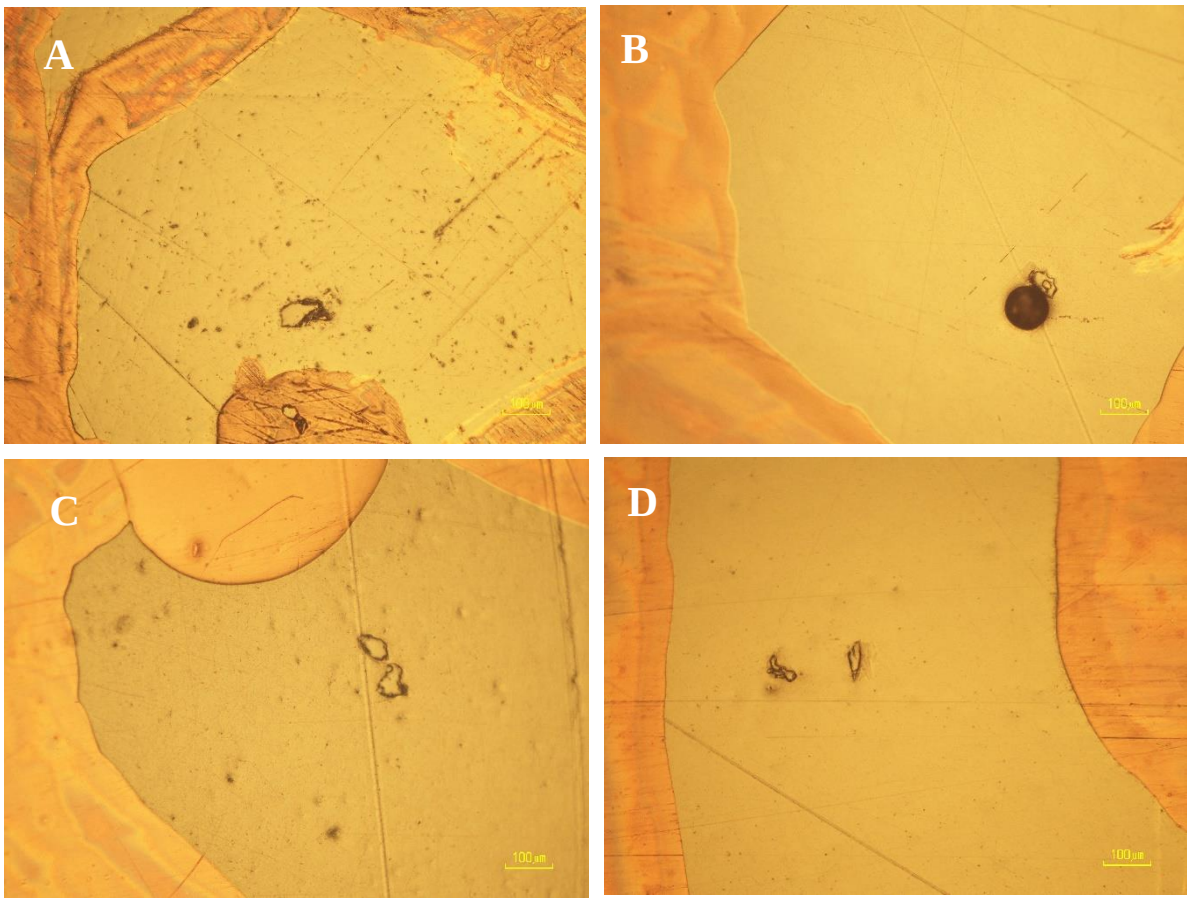

*Figure 4: Cryptotephra found at Whitney Mesa; **A**: WM19 - 1; **B**: WM19 - 11; **C**: WM19 - 12; **D**: WM19 - 13*

Using UNLV's Electron Micro-Imaging Laboratory (EMiL) JEOL SuperProbe (JXA8900R WD/ED Combined Microanalyzer), with a 5-micron electron beam, samples 19WM-1, 11, 12, and 13 were analyzed. All four selected samples were identified as rhyolite shards. Results, normalized water (LOI) free, from the microprobe analysis can be found in Table 1 (raw data results are provided in Appendix 3).

Table 1: Normalized data from Electron Microprobe analyses

	19WM-1	19WM1-2	19WM11	19WM12	19WM13	Mean
SiO_2	77.38	77.32	77.37	77.43	77.09	**77.32**
TiO_2	0.05	0.08	0.01	0.08	0.06	**0.06**
Al_2O_3	12.65	12.77	12.71	12.70	12.56	**12.68**
Cr_2O_3	0.00	0.00	0.00	0.01	0.03	**0.01**
Fe_2O_3	0.59	0.58	0.99	0.64	1.00	**0.76**
MnO	0.05	0.08	0.03	0.05	0.00	**0.04**
MgO	0.00	0.00	0.00	0.15	0.01	**0.03**
CaO	0.56	0.60	0.59	0.53	0.54	**0.56**
Na_2O	3.61	3.52	3.47	3.44	3.75	**3.56**
K_2O	4.94	4.88	4.66	4.73	4.76	**4.79**
Cl	0.12	0.14	0.21	0.17	0.04	**0.14**
SO_3	0.04	0.06	0.00	0.11	0.16	**0.07**
BaO	0.06	0.00	0.00	0.00	0.02	**0.02**
Total Before Normalization	96.23	95.12	97.78	95.8	96.7	**96.23**

Of these chemical components, the mean normalized wt. % SiO_2 is 77.32 and Al_2O_3 12.68 wt. %, indicating a rhyolitic composition. This aids in the comparison of potential correlative events. Further trends observed include iron oxide content remaining below 1.00 wt. % and the K_2O/Na_2O ratio having a mean value of 1.346.

Tephra Correlation

To determine the volcanic source for these cryptotephra, we compared our geochemical analyses with data from known samples of the specific tephra deposits chosen as potential correlations: Rockland, Loleta, Lava Creek B, and Bishop Tuff (Figure 5) (Sarna-Wojcicki et al., 1985; Pouget et al., 2014; Sarna-Wojcicki et al., 1987; Maier et al., 2015). When compared, our samples most closely align with Bishop Tuff data (Table 2, Figures 6-9). Unlike other Western United States events of similar ages, Bishop Tuff and the cryptotephra found at Whitney Mesa all have a lower iron content, close to 0.76 wt. %, which therefore negatively correlates with any events of higher iron content such as Lava Creek B (Figure 7). Our Whitney Mesa samples also had similar wt. % of manganese, magnesium, and calcium to reported Bishop Tuff values.

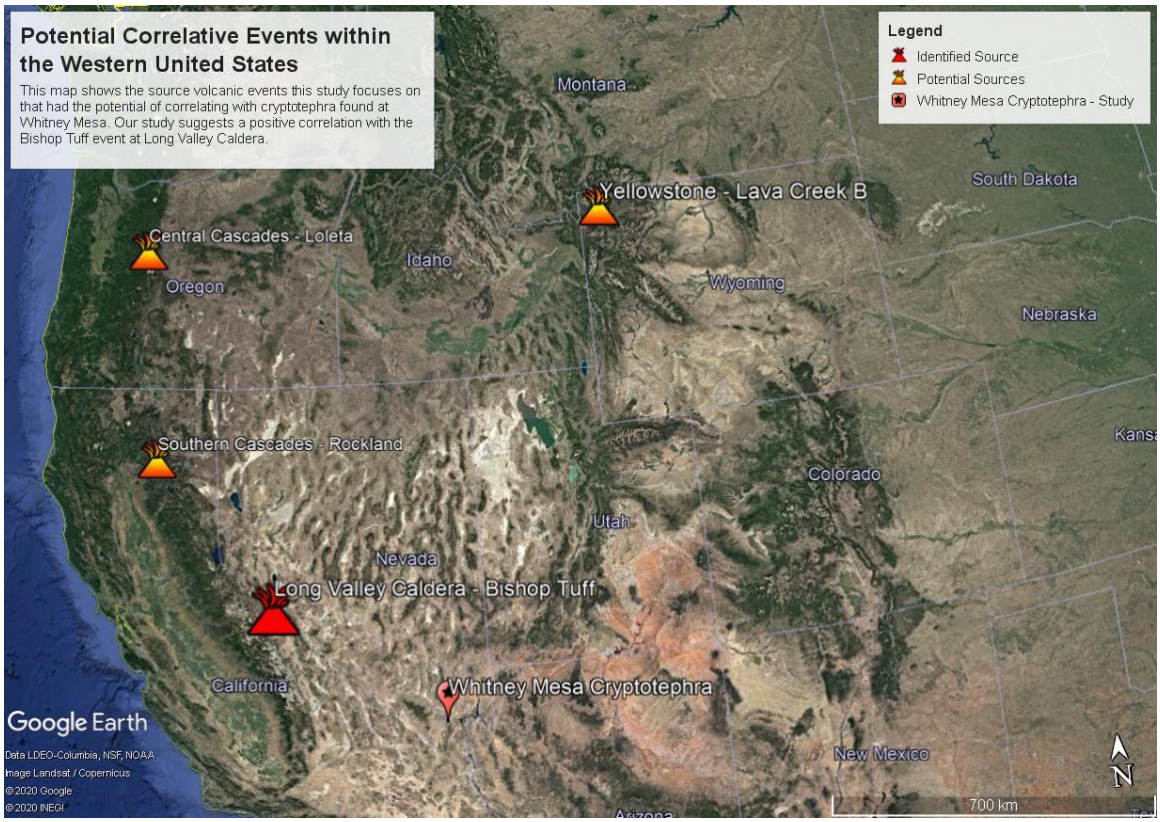

Figure 5: Map of potential correlative events within the Western US, made using Google Earth

The ratio between potassium and sodium are also similar, with the average ratio for Whitney Mesa being calculated as 1.346 and that of Bishop Tuff 1.292, differing from the other events (Rockland, 0.9572; Lava Creek B, 1.438; Loleta, 0.6422). It is seen that Lava Creek B and Whitney Mesa share similar manganese, magnesium, and calcium values; however, the potassium to sodium ratio differs and the iron content for Lava Creek B is significantly higher than that of Whitney Mesa.

Table 2: Geochemical data for correlation between various western US volcanic complexes

	Whitney Mesa	**Rockland** (Sarna Wojcicki et al., 1985)	**Lava Creek B** (Pouget et al., 2014)	**Bishop Tuff** (Sarna-Wojcicki et al., 1987)	**Loleta Ash** (Maier et al., 2015)
Location	Las Vegas, NV	Southern Cascades, CA	Yellowstone, WY	Long Valley Caldera, CA	Central Cascades, OR
Age (ka)	226-573<<	575	631	766	390
SiO_2	77.32	77.7	76.7	77.55	74.77
TiO_2	0.06	0.16	0.11	0.06	0.154
Al_2O_3	12.68	12.7	12.35	12.64	14.05
Fe_2O_3	0.76	0.92	1.41	0.74	1.92
MnO	0.04	0.03	0.03	0.03	0.064
MgO	0.03	0.17	0.03	0.04	0.114
CaO	0.56	0.89	0.53	0.45	0.758
Na_2O	3.56	3.74	3.56	3.7	4.98
K_2O	4.79	3.58	5.12	4.78	3.198

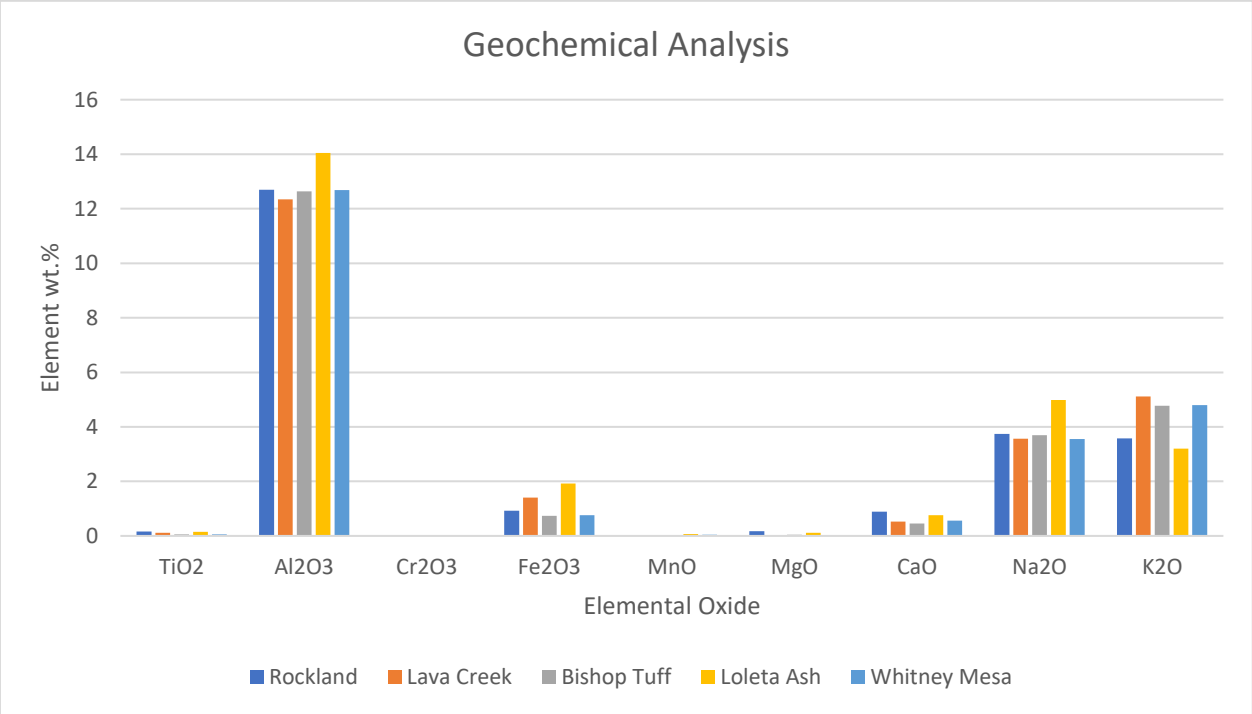

Figure 6: Chart comparing potential correlations across western US volcanic events

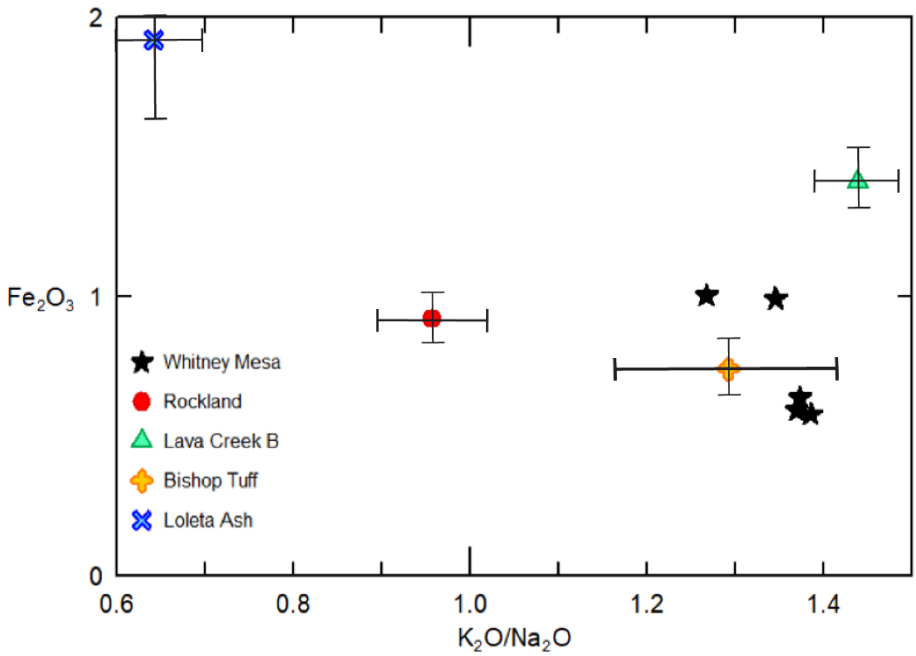

Figure 7: Comparison of Fe and K:Na data between Whitney Mesa and potential correlative events

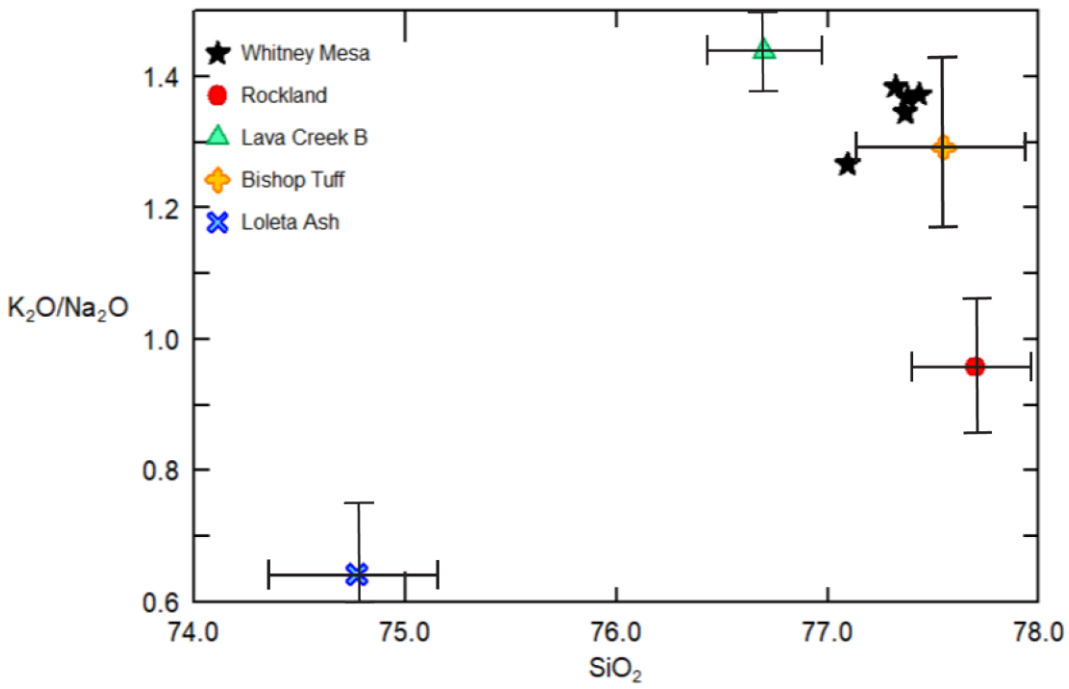

Figure 8: Comparison of K, Na, and Si data between Whitney Mesa and other potential correlative events.

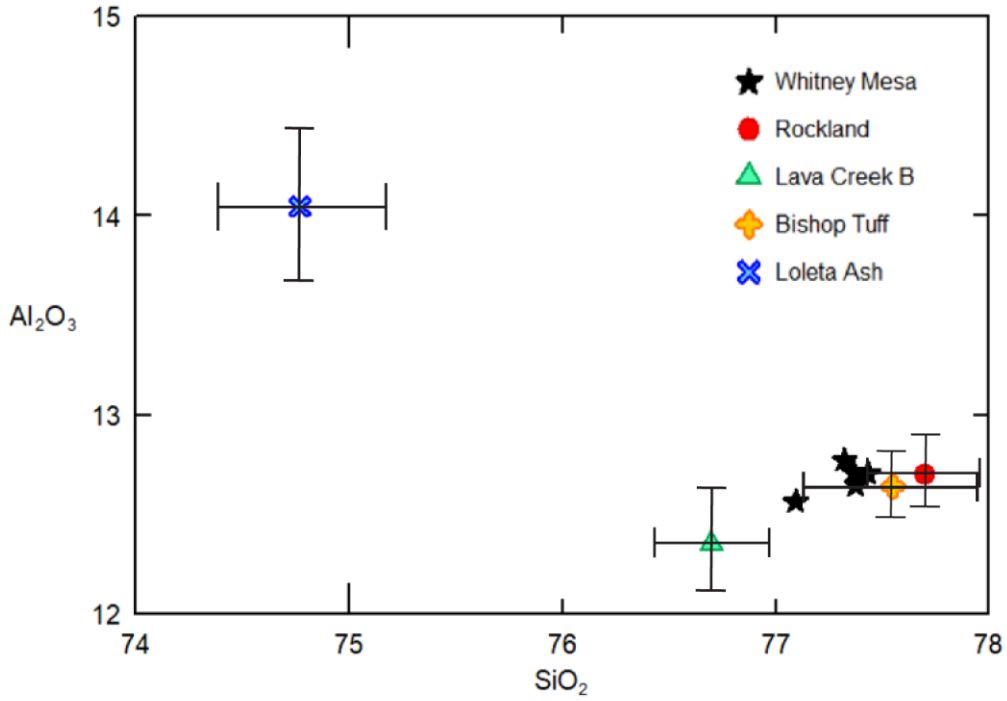

Figure 9: Comparison of Si and Al data between Whitney Mesa and other potential correlative events.

Discussion

Shard Distribution

It should also be noted here that three of the shards (19WM-11, 12, and 13) were found in stratigraphic succession while the shard from sample 19WM-1 was found near the base of the escarpment, a meter below sample 19WM-11 (Figure 10). This basal section was dominated by debris fall and reworked sediments, making any collections less than ideal and more likely to contain debris material. Since no shards were found in samples 2-9, and remobilized sediment was observed from weathering and erosional processes, it is likely that this shard is originally from higher up in the stratigraphic column, closer to where 19WM-11, 19WM-12, and 19WM-13 were found. Debris fall, gravity, rain, and other processes may have contributed to its remobilization.

Figure 10: Collection cliff face and points of cryptotephra discovery

Distribution area of the Bishop Tuff

Whitney Mesa lies well within the distribution area of the Bishop Tuff (Figure 11) (Izett et al., 1982 and 1988), which erupted at 766 ka and formed Long Valley Caldera in eastern California (Izett et al., 1988). Creating the 15x30 km caldera and producing 500-600 km^3 of ash projected to cover over 1 million km^2 of the Western U.S., this volcanic event was catastrophic (Izett et al., 1988.). This system remains seismically and geothermally active, with active fumaroles and hot springs, while also acting as the power source for 40,000 homes in California (Volcano Hazards Program U.S.G.S.).

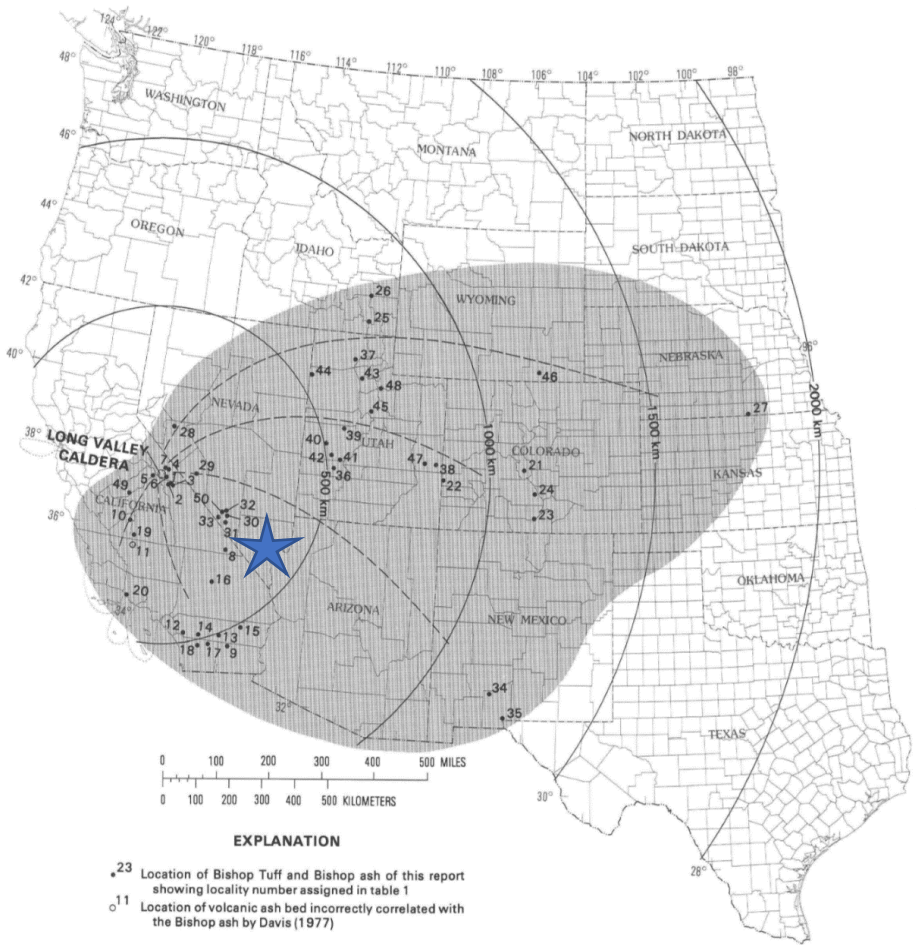

Figure 11: Distribution of Bishop Tuff taken from page 4 of Izett et al., 1988. Star represents Las Vegas, Nevada.

The discovery of Bishop Tuff in Bed X2 of Unit X provides a precise date for the Las Vegas Formation at Whitney Mesa. Previously, the only reported dates for Unit X were 399-226 ka, 379-232 ka (Lundstrom et al., 1998; Page et al., 2005) and those of Springer et al. (2018) 573 ± 52 ka, all from Bed X4 of Unit X. This study provides the first date for Bed X2 in the middle-lower part of the section.

Conclusions

Cryptotephra is a key dating tool used in archaeological, palaeoclimatological, and geohazard studies due to its narrow isochron and its links to transportation and depositional processes. The study of cryptotephra is an expanding field that can be used globally thanks to the range of potential preservation sites and the small particulate size allowing cryptotephra to travel thousands of kilometers from its source volcano. This study found and analyzed four cryptotephra shards at Whitney Mesa within the Las Vegas Formation's Unit X using wet-lab techniques at UNLV's CLAGR and electron microprobe analysis at UNLV's EMiL. The rhyolitic shards were positively correlated with the 766 ka Bishop Tuff, from an event which formed the Long Valley Caldera in California. These results add a more accurate time constraint to Las Vegas Formation Unit X. It is suggested that further studies may be conducted to use Bishop Tuff shards to correlate other sediments and members to Unit X, such as the Chemehuevi Formation dated at <780 ka ((Kukla, 1975; Bell et al., 1978; Lundstrom et al., 2008) in Malmon et al., 2011) as well as to consider further study of the Las Vegas Formation concerning preservation processes of tephra deposits.

References Cited

Blockley, S.P.E., Pyne-O'Donnell, S.D.F., Lowe, J.J., Matthews, I.P., Stone, A., Pollard, A.M, Turney, C.S.M., & Molyneux, E.G., 2005, A new and less destructive laboratory procedure for the physical separation of distal glass tephra shards from sediments: Quaternary Science Reviews, p. 1952-1960

Blockley, S.P.E., Ramsey, C.B., & Pyle, D.M, 2007, Improved age modelling and high-precision age estimates of late Quaternary tephras, for accurate palaeoclimate reconstruction: Journal of Volcanology and Geothermal Research, Vol. 177, p. 251-262

Chen, X., McLean, D., Blockley, S.P.E., Tarasov, P.E., Xu, Y., & Menzies, M.A., 2019, Developing a Holocene tephrostratigraphy for northern Japan using the sedimentary record from Lake Kushu, Rebun Island: Quaternary Science Reviews, Vol. 215, p. 272-292, doi.org/10.1016/j.quascirev.2019.05.017

Davies, L.J., Appleby, P., Jensen, B.J.L., Magnan, G., Mullan-Boudreau, G., Noernberg, T., Shannon, B., Shotyk, W., van Bellen, S., Zaccone, C., & Froese, D.G., 2018, High-resolution age modelling of peat bogs from northern Alberta, Canada, using pre- and post-bomb ^{14}C, ^{210}Pb and historical cryptotephra: Quaternary Geochronology, Vol. 47, p. 138-162, doi:10.1016/j.quageo.2018.04.008

D'Andrea, W.J., Vaillencourt, D.A., Balascio, N.L., Werner, A., Roof, S.R., Retelle, M., & Bradley, R.S., 2012, Mild Little Ice Age and unprecedented recent warmth in an 1800-year lake sediment record from Svalbard: Geology, Vol. 40., No. 11, doi.org/10.1130/G33365.1

dePolo, C.M, Taylor, W.J., Burns, S., Middleton, L.T., & Metcalf, R.V., 2008, Characterizing the earthquake potential of the Las Vegas Valley fault system: Geological Society of America, Vol. 40, No.1. p. 72

Folch, A., 2012, A review of tephra transport and dispersal models: Evolution, current status, and future perspectives: Journal of Volcanology and Geothermal Research, Vol. 235-236, p. 96-115, doi:10.1016/j.jvolgeores.2012.05.020

Giaccio, B., Niespolo, E.M., Pereira, A., Nomade, S., Renne, P.R., Albert, P.G., Arienzo, I., Regattieri, E., Wagner, B., Zanchetta, G., Gaeta, M., Galli, P., Mannella, G., Peronace, E., Sottili, G., Florindo, F., Leicher, N., Marra, F., & Tomlinson, E.L., 2017, First integrated tephrochronological record for the last ~190 kyr from the Fucino Quaternary lacustrine succession, central Italy: Quaternary Science Reviews, Vol. 158, p. 211-234, doi: 10.1016/j.quascirev.2017.01.004

Herrick, J.A., Jacques, K.D., Landowski, C.M., Shields, D.A., & Stamm, N.R., 2018, Geologic Nomenclature and Description: U.S. Geological Survey Draft, version 1.0.

Hirniak, J.N., Smith, E.I., Johnsen, R., Ren, M., Hodgkins, J., Orr, C., Negrino, F., Riel-Salvatore, J., Fitch, S., Miller, C.E., Zerboni, A., Mariani, G.S., Harris, J.A., Gravel-Miguel, C., Strait, D., Peresani, M., Benazzi, S, & Marean, CW., 2020, Discovery of cryptotephra at Middle-Upper Paleolithic sites Arma Veirana and Riparo Bombrini, Italy: a new link for broader geographic correlations: Journal of Quaternary Science, doi:10.1002/jqs.3158

Hurford, A.J., & Hammerschmidt, K., 1985, $^{40}Ar/^{39}Ar$ and K/Ar dating of the Bishop and Fish Canyon tuffs: Calibration ages for fission-track dating standards: Isotope Geoscience section, Vol. 58, No. 1-2, p. 23-32.

Izett, G.A., 1981, Volcanic Ash Beds: Recorders of Upper Cenozoic Silicic Pyroclastic Volcanism in the Western United States; Journal of Geophysical Research, Vol. 86, No. B11, p.10200-10222

Izett, G.A., Obradovich, J.D., & Mehnert, H.H., 1982, The Bishop Ash Bed and Some Older Chemically and Mineralogically Similar Ash Beds in California, Nevada, and Utah: U.S.

Izett, G.A., Obradovich, J.D., & Mehnert, H.H., 1988, The Bishop Ash Bed (Middle Pleistocene) and Some Older (Pliocene and Pleistocene) Chemically and Mineralogically Similar Ash Beds in California, Nevada, and Utah: U.S.G.S., Department of the Interior

Jenkins, S., Wilson, T., Magill, C., Miller, V., Stewart, C., Blong, R.J., Marzocchi, W., Boulton, M., Bonadonna, C., & Costa, A., 2015, Volcanic ash fall hazard and risk; Global Volcano Model & International Association of Volcanology and Chemistry of the Earth's Interior, Technical background paper for the UN-ISDR Global Assessment Report on Disaster Risk Reduction, doi: 10.1017/CBO9781316276273.005

Kelleher, P.C., & Cameron, K.L., 1990, The Geochemistry of the Mono Craters – Mono Lake Islands Volcanic Complex, eastern California: Journal of Geophysical Research: Solid Earth, Vol. 95, No. B11. DOI: https://doi.org/10.1029/JB095iB11p17643

King, H.M. "Volcanic Explosivity Index (VEI)" Geology.com. https://geology.com/stories/13/volcanic-explosivity-index/

Knott, J.R., Machette, M.N., Wan, E., Klinger, R.E., Liddiocoat, J.C., Sarna-Wojcicki, A.M., Fleck, R.J., Deino, A.L., Geissman, J.W., Slat, J.L., Wahl, D.V., Wernicke, B.P., Wells, S.G., Tinsley, J.C.III, Hathaway, J.C., & Weamer, V.M., 2018, Late Neogene-Quaternary tephrochronology, stratigraphy, and paleoclimate of Death Valley, California, USA: GSA Bulletin, 130(7-8), p. 1231-1255.

Lane, C. S., Cullen, V. L., White, D., Bramham-Law, C. W. F., and Smith, V. C., 2014, Cryptotephra as a dating and correlation tool in archaeology: Journal of Archaeological Science, Vol. 42, p. 42-50.

Lane, C.S., Lowe, D.J., Blockley, S.P.E., Suzuki, T., & Smith, V.C., 2017, Advancing tephrochronology as a global dating tool: Applications in volcanology, archaeology, and paleoclimatology: Quaternary Geochronology, DOI: https://doi.org/10.1016/j.quageo.2017.04.003

Long Valley Caldera and Mono-Inyo Craters Volcanic Field, California: http://volcano.oregonstate.edu/oldroot/volcanoes/volc_images/north_america/california/long_valley.html

Lowe, D.J., 2011, Tephrochronology and its application: A review: Quaternary Geochronology, Vol. 6, No. 2, p. 107-153.

Lowe, D.J., Pearce, N.J.G., Jorgensen, M.A., Kuehn, S.C., Tryon, C.A., & Hayward, C.L., 2017, Correlating tephras and cryptotephras using glass compositional analyses and numerical and statistical methods: Review and evaluation: Quaternary Science Reviews, Vol. 175, p. 1-44.

Luckow, H.G., Pavlis, T.L, Serpa, L.F., Guest, B., Wagner, D.L., Snee, L., Hensley, T.M., & Korjenkov, A., 2005, Late Cenozoic sedimentation and volcanism during transtensional deformation in Wingate Wash and the Owlshead Mountains, Death Valley: Earth-Science Reviews, Vol. 73, p. 177-219.

Lundstrom, S.C., Page, W.R., Langenheim, V.E., Young, O.D., Mahan, S.A., & Dixon, G.L., 1998, Preliminary geologic map of the Valley quadrangle, Clark County, Nevada: U.S. Geological Survey Open-File Report 98-508.

Maier, K.L., Gattie, E., Wan, E., Ponti, D.J., Pagenkopp, M., Staratt, S.W., Olson, H.A., & Tinsley, J.C., 2015, Quaternary tephrochronology and deposition in the subsurface Sacramento-San Joaquin Delta, California, U.S.A.: Quaternary Research, Vol. 83, p. 378-393.

Marcaida, M., Mangan, M.T., Vazquez, J.A., Bursik, M., & Lidzbarski, M.I., 2014, Geochemical fingerprinting of Wilson Creek formation tephra layers (Mono Basin, California) using titanomagnetite compositions: Journal of Volcanology and Geothermal Research, Vol. 273, p. 1-14.

Marcaida, M., Vazquez, J.A., Stelten, M.E., & Miller, J.S., 2019, Constraining the early eruptive history of the Mono Craters Rhyolites, California, based on ^{238U}-^{230Th} isochron dating of their explosive and effusive products: Geochemistry, Geophysics, Geosystems, Vol. 20, p. 1539-1556. DOI: https://doi.org/10.1029/2018GC008052

Malmon, K.V., Howard, K.A., House, P.K., Lundstrom, S.C., Pearthree, P.A., Sarna-Wojcicki, A.M., Wan, E., & Wahl, D.B., 2011, Stratigraphy and Depositional

Environments of the Upper Pleistocene Chemehuevi Formation Along the Lower Colorado River: United States Geological Survey, Professional Paper 1786

Mark, D.F., Petraglia, M., Smith, V.C., Morgan, L.E., Barfod, D.N., Ellis, B.S., Pearce, N.J., Pal, J.N., & Korisettar, R., 2014, A high-precision $^{40}Ar/^{39}Ar$ age for the Young Toba Tuff and dating of ultra-distal tephra: Forcing of Quaternary climate and implications for hominin occupation of India: Quaternary Geochronology, Vol. 21, p. 90-103, doi:10.1016/j.quageo.2012.12.004

Mark, D.F., Renne, P.R., Dymock, R.C., Smith, V.C., Simon, J.I., Morgan, L.E., Staff, R.A., Ellis, B.S., & Pearce, N.J.G., 2017, High-precision 40Ar/39Ar dating of Pleistocene tuffs and temporal anchoring of the Matuyama-Brunhes boundary: Quaternary Geochronology, Vol. 39, p. 1-23.

Martin-Jones, C.M., Lane, C.S., Pearce, N.J.G., Smith, V.C., Lamb, H.F., Schaebitz, F., Viehberg, F., Brown, M.C., Franke, U., & Asrat, A., 2017, Recurrent explosive eruptions from a high-risk Main Ethiopian Rift volcano throughout the Holocene: Geology, Vol. 45, No. 12, doi.org/10.1130/G39594.1

Matthews, N.E., Vazquez, J.A., & Calvert, A.T., Age of the Lava Creek supereruption and magma chamber assembly at Yellowstone based on $^{40}Ar/^{39}Ar$ and U-Pb dating of sanidine and zircon crystals: Geochemistry, Geophysics, Geosystems, Vol. 16, No. 8, 2015. Doi: 10.1002/2015GC005881

McCanta, M.C., Hatfield, R.G., Thomson, B.J., Hook, S.J., & Fisher, E., 2015, Identifying cryptotephra units using correlated rapid, nondestructive methods: VSWIR spectroscopy, X-ray fluorescence, and magnetic susceptibility: Geochemistry, Geophysics, Geosystems, Vol. 16., No.12, p. 4029-4056.

Page, W.R., Lundstrom, S.C., Harris, A.G., Langenheim, V.E., Workman, J.B., Mahan, S.A., Paces, J.B., Dixon, G.L., Rowley, P.D., Burchfiel, B.C., Bell, J.W., & Smith, E.I., 2005, Geologic and geophysical maps of the Las Vegas 30' x 60' quadrangle, Clark and Nye Counties, Nevada, and Inyo County, California: U.S. Geological Survey Report 2814. DOI: https://doi.org/10.3133/sim2814

Parker, G., 2013, Global Crisis: War, Climate Change and Catastrophe in the Seventeenth Century; New Haven, Yale University Press, p. 15

Pouget, S., Bursik, M., Cortes, J.A., & Hayward, C., 2014, Use of principal component analysis for identification of Rockland and Trego Hot Springs tephras in the Hat Creek Graben, northeastern California, USA: Quaternary Research, Vol. 81, No. 1, p. 125-137.

Rampino, Michael R.; Self, Stephen, 1992, "Volcanic Winter and Accelerated Glaciation following the Toba Super-eruption." Nature. Vol. 359, p. 50–52.

Rowland, S.M., Parry, L.E., & Anon., 2015, Age profile of terminal Pleistocene Columbian mammoths from the Tule Springs fossil beds of southern Nevada: Geological Society of America Abstract, Vol. 47, No. 7, p. 138

Sarna-Wojcicki, A.M., Bowman, H.R., Meyer, C.E., Russell, P.C., Woodward, M.J., Rowe, G.M.J.J., Baedecker, P.A., Asaro, F., & Michael, H., 1984, Chemical analyses, correlations, and ages of upper Pliocene and Pleistocene ash layers of East-Central and Southern California: U.S. Geological Survey Professional Paper, No. 1293. DOI: https://doi.org/10.3133/pp1293

Sarna-Wojcicki, A.M., Meyer, C.E., Bowman, H.R., Hall, N.T., Russell, P.C., Woodward, M.J., & Slates, J.L., 1985, Correlation of the Rockland Ash Bed, a 400,000-Year-Old Stratigraphic Marker in Northern California and Western Nevada, and Implications for Middle Pleistocene Paleogeography of Central California: Quaternary Research 23, p. 236-257

Schmincke, H., 2004, Volcanism: Springer-Verlag Berlin Heidelberg, p. X-324, doi:10.1007/978-3-642-18952-4

Sellards, E.H., 1960, Some Early Stone Artifact Developments in North America: The University of Chicago Press, Vol. 16, p. 160-173

Simpson, G.G., 1933, A Nevada Fauna of Pleistocene Type and its Probable Association with Man: American Museum Novitates, no. 667

Smith, E.I., Jacobs, Z., Johnsen, R., Ren, M., Fisher, E.C., Oestmo, S. Wilkins, J., Harris, J.A., Karkanas, P., Fitch, S., Ciravolo, A., Keenan, D., Cleghorn, N., Lane, C.S., Matthews, T., & Marean, C.W., 2018, Humans thrived in South African through the Toba eruption about 74,000 years ago: Nature, Vol. 555, p. 511-515, doi:10.1038/nature25967.

Smith, E. I., Rowland, S. M., Johnsen, R., Ren, M., and Fitch, S., 2019, First report of cryptotephra from the Las Vegas Formation, Tule Springs Fossil Beds National Monument, Nevada, Geological Society of America, Volume Abstract 55-7: Phoenix, Arizona.

Smithsonian Institution, National Museum of Natural History, Global Volcanism Program; http://volcano.si.edu/volcano.cfm?vn=321050

Springer, K.B., Manker, C.R., Scott, E., Pigati, J., & Mahan, S.A., 2015, The geology, paleohydrology and fossils of Tule Springs Fossil Beds National Monument, Nevada; a late Pleistocene treasure trove: Geological Society of America, v. 47, No. 7, p. 656.

Springer, K.B., Pigati, J.S., Manker, C.R., & Mahan, S.A., 2018, The Las Vegas Formation: U.S. Geological Survey Professional Paper 1839, p. 62.

Springer, K.B, Pigati, J.S., & Scott, E., 2018, The geology and paleontology of Tule Springs Fossil Beds National Monument, Nevada: U.S. Geological Survey Report, Vol. 4, DOI: 10.3133/fs20183038.

Springer, K., Sagebiel, J.C., Scott, E., Manker, C., & Austin, C., 2005, The Late Pleistocene Vertebrate Paleontology of the Las Vegas Formation, Clark County, Nevada: Division of Geological Sciences, San Bernardino County Museum, Vol. 25, p. 33A

Taylor, W.J., 2003, Influence of Tertiary structures on Quaternary faults, Las Vegas Basin, Nevada: Geological Society of America, Vol. 35, No. 6, p. 476.

Walker, J.D., Geissman, J.W., Bowring, S.A., & Babcock, L.E., 2013, GSA Geologic Time Scale: Geological Society of America Bulletin, p. 259-272.

Wastegard, S., Gudmundsdottir, E.R., Lind, E.M., Timms, R.G.O., Bjorck, S., Hannon, G.E., Olsen, J., & Rundgren, M., 2018, Towards a Holocene tephrochronology for the Faroe Islands, North Atlantic: Quaternary Science Reviews, Vol. 195, p. 195-214, doi:10.1016/j.quascirev.2018.07.024

Yang, Q., Bursik, M., & Pitman, E.B., 2019, A new method to identify the source vent location of tephra fall deposits: development, testing, and application to key Quaternary eruptions of Western North America: Bulletin of Volcanology, DOI: https://doi.org/10.1007/s00445-019-1310-0

Vazquez, J.A., & Lidzbarski, M.I., 2012, High-resolution tephrochronology of the Wilson Creek Formation (Mono Lake, California) and Laschamp event using ^{238U}-^{230Th} SIMS dating of accessory mineral rims: Earth and Planetary Science Letters, p. 357-358.

Zanchetta, G., Sulpizio, R., Cioni, Eastwood, W.J., Siani, G., Caron, B., Paterne, M., & Santacroce, R., 2011, Tephrostratigraphy, chronology and climatic events of the Mediterranean basin during the Holocene: An overview: The Holocene, doi: 10.1177/0959683610377531

Zeeden, C., Rivera, T.A., Storey, M., 2014, An astronomical age for the Bishop Tuff and concordance with radioisotopic dates: Geophysical Research Letters, v. 41, 3478-3484: doi:10.1002/ 2014GL059899.

Appendix 1 – Transportation Processes [VEI]

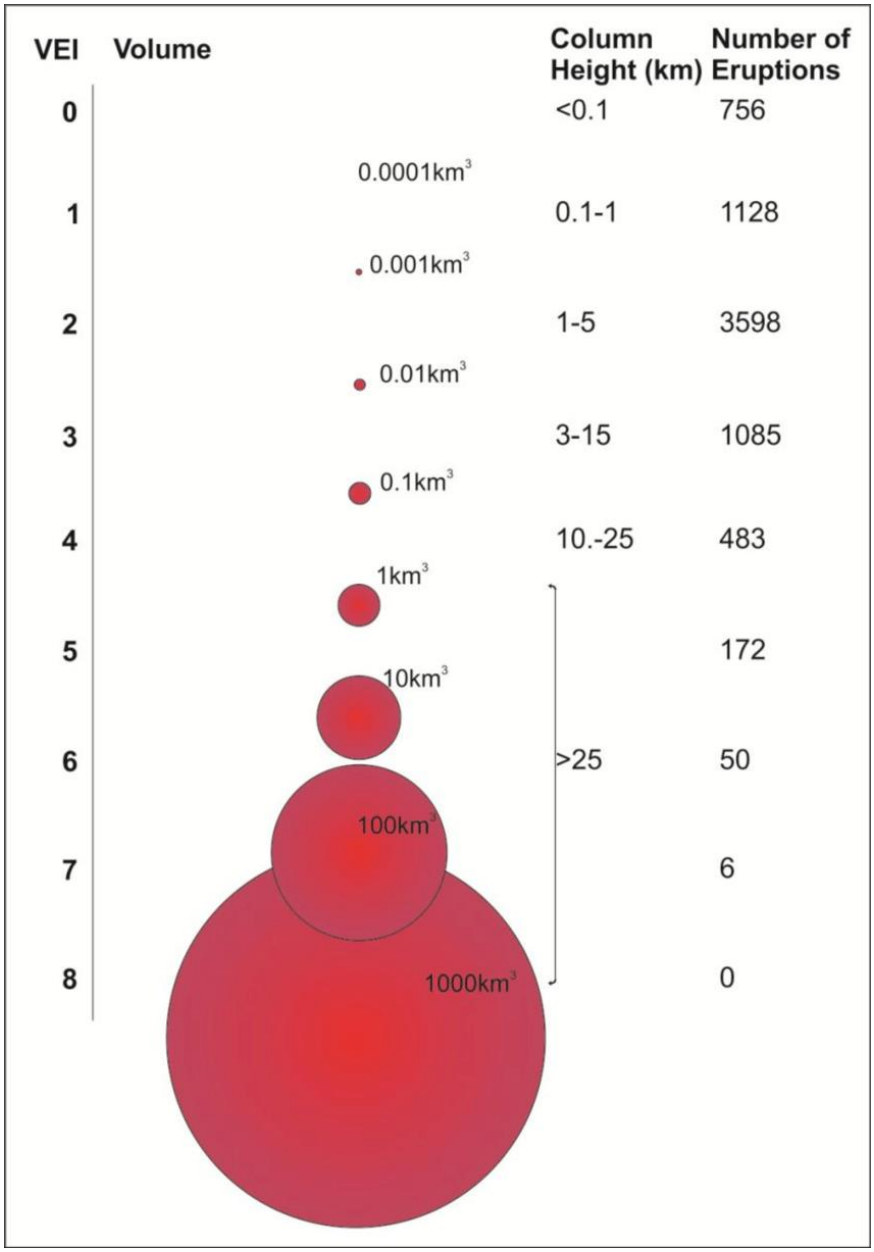

Volcanic Explosivity Index figure taken from Jenkins et al., 2015.

Appendix 2 – Processing Methods Flow Chart

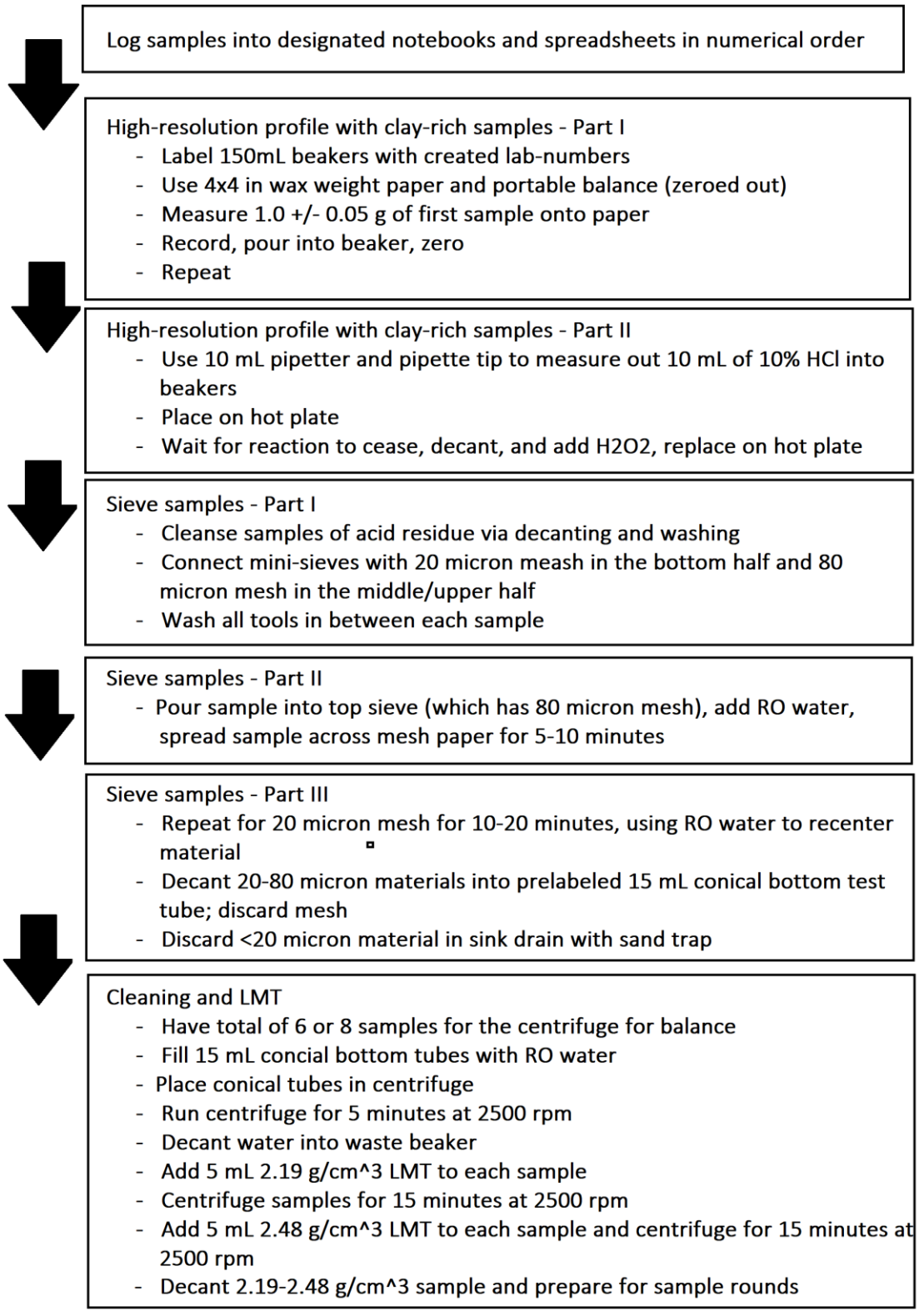

Appendix 3 – Results [Raw Data]

	19WM1-1	19WM1-2	19WM11	19WM12	19WM13
SiO_2	74.46	73.55	75.65	74.18	74.55
TiO_2	0.05	0.08	0.01	0.08	0.06
Al_2O_3	12.17	12.15	12.43	12.17	12.15
Cr_2O_3	0	0	0	0.01	0.03
Fe_2O_3	0.57	0.55	0.97	0.61	0.97
MnO	0.05	0.08	0.03	0.05	0
MgO	0	0	0	0.14	0.01
CaO	0.54	0.57	0.58	0.51	0.52
Na_2O	3.47	3.35	3.39	3.3	3.63
K_2O	4.75	4.64	4.56	4.53	4.6
Cl	0.12	0.13	0.21	0.16	0.04
SO_3	0.04	0.06	0	0.11	0.15
Bao	0.06	0	0	0	0.02
Total	96.23	95.12	97.78	95.8	96.7